DR. HEUNG-CHIN CHENG (Orcid ID : 0000-0002-4965-7148)

Article type : Original Article

The Roc-COR Tandem Domain of Leucine-Rich Repeat Kinase 2 (LRRK2) Forms Dimers and Exhibits Conventional Ras-Like GTPase Properties

Ryan D. Mills[2,3§], Lung-Yu Liang[1,2,3§], Daisy Sio-Seng Lio[1,2,3], Yee-Foong Mok[2,3], Terrence D. Mulhern[2,3], George Cao[2,3], Michael Griffin[2,3], Vijaya Kenche[3,4], Janetta G. Culvenor[5] and Heung-Chin Cheng[1,2,3]

§R. D. Mills and L.-Y. Liang contributed equally to this manuscript.

[1]Cell Signaling Research Laboratories, [2]Department of Biochemistry and Molecular Biology, [3]Bio21 Institute of Molecular Science and Biotechnology, University of Melbourne, [4]Florey Neuroscience Institute, and [5]Department of Pathology, University of Melbourne, Parkville, Victoria 3010, Australia

Send all correspondence to:
Heung-Chin Cheng.
Department of Biochemistry and Molecular Biology, University of Melbourne, Parkville, Victoria 3010, Australia.
Ph: (+613)-83442254; E-mail: heung@unimelb.edu.au

This is the author manuscript accepted for publication and has undergone full peer review but has not been through the copyediting, typesetting, pagination and proofreading process, which may lead to differences between this version and the Version of Record. Please cite this article as doi: 10.1111/jnc.14566

Key words: Parkinson's disease, GTPase, protein kinase, Leucine-rich repeat kinase 2, Roco-family proteins

ABSTRACT

The Parkinson's disease (PD)-causative leucine-rich repeat kinase 2 (LRRK2) belongs to the Roco family of G-proteins comprising a Ras-of-complex (Roc) domain followed by a C-terminal of Roc (COR) domain in tandem (called Roc-COR domain). Two prokaryotic Roc-COR domains have been characterized as "G proteins activated by guanine nucleotide-dependent dimerization" (GADs), which require dimerization for activation of their GTPase activity and bind guanine nucleotides with relatively low affinities. Additionally, LRRK2 Roc domain in isolation binds guanine nucleotides with relatively low affinities. As such, LRRK2 GTPase domain was predicted to be a GAD. Herein, we describe the design and high-level expression of human LRRK2 Roc-COR domain (LRRK2 Roc-COR). Biochemical analyses of LRRK2 Roc-COR reveal that it forms homodimers, with the C-terminal portion of COR mediating its dimerization. Furthermore, it co-purifies and binds Mg^{2+}GTP/GDP at 1:1 stoichiometry, and it hydrolyzes GTP with K_m and k_{cat} of 22 nM and 4.70×10^{-4} min^{-1}, respectively. Thus, even though LRRK2 Roc-COR forms GAD-like homodimers, it exhibits conventional Ras-like GTPase properties, with high affinity binding of Mg^{2+}-GTP/GDP and low intrinsic catalytic activity. The PD-causative Y1699C mutation mapped to the COR domain was previously reported to reduce the GTPase activity of full-length LRRK2. In contrast, this mutation induces no change in the GTPase activity, and only slight perturbations in the secondary structure contents of LRRK2 Roc-COR. As this mutation does not directly affect the GTPase activity of the isolated Roc-COR tandem, it is possible that the effects of this mutation on full-length LRRK2 occur via other functional domains.

(Word count: 249)

INTRODUCTION

Human LRRK2, encoded by the Parkinson's disease (PD)-causative *LRRK2* gene, is a large protein of 2527 amino acids consisting of 7 predicted domains: an N-terminal armadillo repeat domain, an ankyrin repeat domain, a leucine-rich repeat (LRR) domain, a Ras-like GTPase domain (Roc, Ras of complex proteins), a COR (C-terminal of Roc) domain, a protein kinase domain, and a WD-40 repeat domain (Mills *et al.* 2014, Mata *et al.* 2006). The arrangement of LRR, Roc, COR and kinase domains is typical of Roco family proteins, found in eukaryotic and prokaryotic species (Bosgraaf & Van Haastert 2003, Marin *et al.* 2008). All Roco family members contain a Roc domain followed by a C-terminal COR domain (Bosgraaf & Van Haastert 2003, Marin et al. 2008). Structural and biochemical analyses of two prokaryotic Roco proteins revealed that the Roc and COR domains form extensive inter-domain interactions to govern dimerization and catalytic properties of their GTPase activity (Gotthardt *et al.* 2008, Terheyden *et al.* 2015). As such, the Roc and COR domains are considered to act as a single functional unit, which is referred to as the Roc-COR tandem domain.

Dysregulation of the Roc GTPase domain of LRRK2 is implicated in PD pathogenesis because of the prevalent PD-causative R1441C/G/H mutations mapped to this domain; these mutations lead to decreased GTPase activity (Floris *et al.* 2009, Matta *et al.* 2012, Paisan-Ruiz *et al.* 2004). In addition to altering GTPase activity, the R1441H mutation also perturbs the thermal stability of the LRRK2 Roc domain when bound to guanine nucleotides or their analogs (Liao *et al.* 2014, Li *et al.* 2009). Emerging evidence suggests the Roc domain may be central to LRRK2 function, possibly exerting a regulatory influence on the kinase domain [reviewed in (Terheyden *et al.* 2016)]. LRRK2 forms homodimers in cells, and purified recombinant full-length LRRK2 forms dimers in solution (Civiero *et al.* 2012, Guaitoli *et al.* 2016, Klein *et al.* 2009, Sejwal *et al.* 2017). Furthermore, LRRK2 is known to form heterodimers with Leucine Repeat Rich Kinase 1 (LRRK1) and Death-Associated Protein Kinase 1 (DAPK1) (Dachsel *et al.* 2010, Klein et al. 2009). This suggests LRRK2 enzymatic regulation could similarly occur in *trans*, between neighboring LRRK2 subunits or between LRRK2 and its neighboring binding partners, and hence dimerization may be crucial for governing GTPase activity (Guaitoli

et al. 2016). However, further exploration of this possibility has been hampered by low expression levels of recombinant human LRRK2.

Study of human LRRK2 has been benefited by comparison with prokaryotic homologues. A crystal structure of the nucleotide-free state of Roc and COR domains of a prokaryotic Roco family member expressed in the bacterium *C. tepidum* showed that the COR domain comprises two globular subdomains (Gotthardt et al. 2008). Deyaert, *et al.* demonstrated that *C. tepidum* Roc-COR protein forms dimers when it is in the nucleotide-free state or complexed with Mg^{2+}-GDP but forms monomers when complexed with Mg^{2+}-GTP. Furthermore, its transition between the dimeric and monomeric states is a dynamic process governed by GTP turnover (Deyaert *et al.* 2017).

The molecular basis of enzymatic regulation in LRRK2 and its prokaryotic homologs has yet to be comprehensively defined. However, previous findings have supported a possible functional similarity with the family of G-proteins activated by dimerization (GADs) [reviewed in (Nixon-Abell *et al.* 2016, Gasper *et al.* 2009)]. In order to efficiently catalyze GTP hydrolysis, GADs require intermolecular interactions between dimeric units to assemble the active site appropriately for efficient catalysis. GADs are also distinguished from other GTPases by their much lower affinities for guanine nucleotides (with K_D in the µM range) [refer to (Wittinghofer & Vetter 2011) for review]. Results of biochemical and structural analyses of the Roc-COR domains of Roco proteins from prokaryotes *C. tepidum* and *M. barkeri* confirm that they possess properties of GADs (Terheyden et al. 2015, Gotthardt et al. 2008). A role for dimerization in catalytic regulation, as observed for GADs, is supported by the ability of full-length human LRRK2 and LRRK2 Roc domain to form dimers in solution (Sen *et al.* 2009, Ito & Iwatsubo 2012, Liao et al. 2014, Sejwal et al. 2017, Guaitoli et al. 2016) and the low affinities exhibited by LRRK2 Roc domain for GDP and a GTP analog (K_D ~ 3-7 µM) (Liao et al. 2014).

Because of the technical challenges posed by expressing sufficient quantities of high quality recombinant human LRRK2 Roc-COR tandem domain, one of our objectives is to overcome these challenges to express a recombinant protein consisting of this LRRK2 tandem domain for detailed biochemical analyses and future structural

studies. Specifically, we have addressed three key questions: (i) What is the appropriate LRRK2 construct suitable for high level expression and purification of active recombinant LRRK2 Roc-COR tandem domain? (ii) Does the recombinant protein consisting of just the LRRK2 Roc-COR tandem domain functions as a GAD or as a conventional Ras-like GTPase? (iii) How does the PD-causative Y1699C mutation impact the structure and catalytic activity of recombinant LRRK2 Roc-COR domain? This manuscript describes the design and expression of a catalytically active recombinant LRRK2 fragment consisting of the Roc-COR tandem domain. Results of our analysis suggest that the Roc-COR tandem domain exhibits both GAD-like and conventional Ras-like GTPase properties – it forms homodimers like GADs and yet functions like the conventional Ras-like GTPases in binding guanine nucleotides and hydrolyzing GTP. Our analysis of the Y1699C mutant of the LRRK2 Roc-COR tandem domain revealed that the mutation has no significant impact on its stability and catalytic activity.

MATERIALS AND METHODS

This study was not pre-registered and that pre-registration was not required.

Materials

The pcDNA3-LRRK2 plasmid for generating LRRK2 Roc-COR was a kind gift of Dr. M. J. Farrer of the University of British Columbia. The gene encoding the LRRK2 (1324-1858) segment was synthesized by Genscript (RRID:SCR_002891). The gene encoding mouse Rac1 (Uniprot ID P63001) with an N-terminal HA tag was synthesized by Bioneer Pacific (Melbourne, Australia). The pGEX6P3 vector and the pBacPAK9 vector were from GE Bioscience (RRID:SCR_000004) and Clontech (RRID:SCR_004423), respectively. The Quick-Change II site directed mutagenesis kit was from Agilent. Grace's medium supplemented with 10% (v/v) fetal bovine serum and Sf-900™ II serum-free medium (Cat. #:10902104) for insect cell culture were purchased from ThermoFisher. The *Spodoptera frugiperda* clone 9 and clone 21 cell lines (*Sf*9 and *Sf*21 cell lines; RR1D: CVCL_0549 and CVCL_0518, respectively) were from ThermoFisher (RRID:SCR_008817); they are not listed as commonly misidentified cell

lines by the International Cell Line Authentication Committee. The glutathione-agarose for purification of GST-LRRK2 Roc-COR was from GE Healthcare (RRID:SCR_000004). Carrier-free [^{32}P] inorganic phosphate was from Perkin-Elmer. GDP, GTP and the sequencing grade trypsin were from Sigma-Aldrich (RRID:SCR_008988). The HPLC instrument (Agilent HPLC-Chip Cube MS Interface from G4240A) was from Agilent Technologies (CA, USA). The mass spectrometer relied on LTQ Orbitrap XL Hybrid Ion Trap-Orbitrap was from Thermo-Fisher (MA, USA). All other chemicals used in our study were of analytical grade. No experimental models were used in this study. Thus, institutional approval for the use of animals was not required.

Plasmids for expression of LRRK2 Roc-COR and short LRRK2 Roc-COR in *E. coli* and baculovirus-infected insect cells

To generate the plasmids for expression of LRRK2 Roc-COR proteins with different affinity tags, we cloned the cDNA encoding the human LRRK2 (1314-1878) segment from the pcDNA3-LRRK2 plasmid by PCR (Supplemental Procedures). For expression of LRRK2 (1314-1878) with different affinity tags in insect cells and/or *E. coli*, the PCR product was subcloned to the pBacPAK9 vector and the pGEX6P3 vector, respectively (Supplemental Procedures).

For expression of the short LRRK2 Roc-COR, the gene encoding the LRRK2 (1324-1858) segment with a poly-His and a Flag tag at the N-terminus and an HA-tag at the C-terminus, was synthesized by Genscript prior to subcloning into the pBacPAK9 vector. The resultant pBacPAK9-LRRK2 (1324-1858) plasmid was used to generate the baculovirus to direct expression of the short LRRK2 Roc-COR protein.

The truncated LRRK2 Roc-CORΔC mutant lacks the C-terminal portion of the COR domain and the linker connecting the COR and kinase domains. For its expression, the gene encoding the LRRK2(1314-1673) segment with a poly histidine tag (His_6) at the C-terminus and a Flag tag at the N-terminus was amplified by PCR. The reaction product was subcloned into the pBacPAK9 vector. The resultant LRRK2 Roc-CORΔC-pBacPAK9 plasmid was used to generate the recombinant baculovirus to direct expression of the LRRK2 Roc-CORΔC mutant.

Purification of GST-LRRK2 Roc-COR expressed in *E. coli* and *Sf*9 cells

Transformed *E. coli* or baculovirus-infected *Sf9* cells were lysed by homogenization in Lysis Buffer (25 mM HEPES, 1 mM EDTA, 0.2 mg/ml benzamidine, 0.1 mg/ml phenylmethylsulfonylfluoride (PMSF), 1 mM β-mercaptoethanol, 0.1 mg/ml soybean trypsin inhibitor (STI), pH 7). For purification from *E. coli*, lysozyme was added to the Lysis Buffer to a final concentration of 0.1 mg/ml to facilitate lysis of the bacterial cell wall. Where *Sf9* cells were used, Lysis Buffer was supplemented with 1 % (v/v) NP-40 to disrupt the cell membrane. Insoluble material was pelleted by centrifugation at 34,540 × g for 20 min at 4 ºC and the supernatant was incubated with glutathione agarose with rocking at 4 ºC for 20 min. The agarose was rinsed with 25 mM HEPES, 1 mM EDTA, 0.2 mg/ml benzamidine, 0.1 mg/ml PMSF, 1 mM β-mercaptoethanol, pH 7, and washed with the same buffer plus 0.5 M NaCl in order to remove non-specifically bound proteins. Proteins bound to the glutathione agarose were eluted with 25 mM HEPES, 0.2 mg/ml benzamidine, 0.1 mg/ml PMSF, 2 mM β-mercaptoethanol, 20 mM glutathione, pH 7 and dialyzed to 25 mM HEPES, 0.1 mg/ ml PMSF, 1 mM β-mercaptoethanol, pH 7.

Generation of recombinant [T1348N]LRRK2 Roc-COR and [Y1699C]LRRK2 Roc-COR

We used the Quick-Change II site-directed mutagenesis kit to generate two mutants of LRRK2 Roc-COR by introducing the T1348N or Y1699C mutations to the pBacPAK9-LRRK2 (1314-1878) plasmid. The resultant plasmids were used to generate the recombinant baculovirus that direct expression of the LRRK2 Roc-COR mutants.

Purification of recombinant LRRK2 Roc-COR and its mutants, and short LRRK2 Roc-COR

For large-scale production (up to 10 mg) of purified recombinant LRRK2 Roc-COR, [Y1699C]LRRK2 Roc-COR, [T1348N]LRRK2 Roc-COR, LRRK2 Roc-CORΔC and short LRRK2 Roc-COR, *Sf9* cells (1 l at a cell density of 0.8-1×10^6 cells per ml) or *Sf*21 (1 l at a cell density of 2-2.5×10^6 cells per ml) were infected with the recombinant baculovirus at an MOI≥1 . At 48 h after infection, the infected insect cells were pelleted

by centrifugation at 1580 × g at 4 ºC. Cell pellets were first re-suspended in 3 ml Lysis Buffer (30 mM Tris, pH 8.0, 150 mM NaCl, 0.1 mg/ ml PMSF and 1 % NP-40) prior to homogenization with a Dounce homogenizer. The homogenate was centrifuged at ~35,000 × g for 20 min at 4 ºC. The supernatant containing the recombinant LRRK2 Roc-COR protein or its mutants was loaded onto a Ni^{2+}-NTA agarose column (10 ml of packed volume). The agarose beads were rinsed with Column Buffer (30 mM Tris, 150 mM NaCl, 0.1 mg/ ml PMSF, pH 8) to remove the unbound proteins. They were subsequently washed with the same buffer supplemented with 30 mM imidazole. Proteins bound to the agarose were eluted in Column Buffer with 300 mM imidazole. The peak protein-containing fractions were pooled and dialyzed in Column Buffer prior to biochemical analysis.

Expression and purification of mouse Rac1

The synthetic gene encoding mouse Rac1 (Uniprot ID P63001) with an N-terminal HA tag was subcloned via the BamH1 and EcoR1 sites to the pGEX6P3 vector directing expression of an N-terminal glutathione S-transferase (GST) tagged recombinant protein. The resultant pGEX6P3 plasmid was used to transform BL21 (DH3) cells. The transformed BL21 (DH3) cells were grown at 37 ^{o}C to a cell density that gave an OD_{600} = 0.5 prior to induction with 0.1 mM isopropyl β-D-1-thiogalactopyranoside (IPTG). The induced cells were cultured further at 16 ºC for 16-18 h before they were harvested by centrifugation at 3000×g for 15 min. The cell pellets were lysed by sonication in Buffer A (10 mM HEPES, 250 mM NaCl, 10 mM $MgCl_2$, 10 mM glycine, 5% glycerol, 2 mM benzamidine, 0.1 mg/ml PMSF, 1 mM β-mercaptoethanol, pH 8.0) supplemented with 10 μM GTP and 1 mg/ml lysozyme to facilitate lysis of the bacterial cell wall. After centrifugation of the homogenate at 35,000×g for 20 min at 4 ^{o}C, the supernatant containing the recombinant GST-HA-Rac1 was incubated for 90 min with glutathione-agarose pre-equilibrated with Buffer A. The GST-HA-Rac1 bound glutathione-agarose was washed with 20 ml Buffer A to remove the non-specifically bound proteins. Buffer A with 20 mM reduced glutathione was used to elute the bound GST-HA-Rac1. The purified proteins were aliquoted and stored at -80 ºC prior to biochemical analyses.

Determination of the secondary structure contents of recombinant LRRK2 Roc-COR and [Y1699C]LRRK2 Roc-COR by circular dichroism spectroscopy

Circular dichroism (CD) spectra were recorded from 5 µM and 300 µl purified LRRK2 Roc-COR and [Y1699C]LRRK2 Roc-COR in a quartz cuvette (1 mm path length) in a temperature-controlled sample chamber attached to a Jasco circular dichroism spectropolarimeter. Spectra were collected from 190 to 260 nm, recording one data point per nm, with a bandwidth of 1 nm and a scanning speed of 20 nm/min. CD spectra were obtained from three independent scans. A representative spectrum was used to estimate secondary structure contents. For secondary structure estimation, data for the range 200 to 250 nm were fitted to the Bestsel prediction program (Micsonai *et al.* 2015) containing reference proteins with varying secondary structures.

Determination of the protein concentrations of the purified recombinant enzymes

Concentrations of the purified proteins we generated were quantified by measurement of the absorbance of the protein preparations at 280 nm and calculation using the molar extinction coefficient of 76320 M^{-1} cm^{-1}, 74830 M^{-1} cm^{-1} and 75033 M^{-1} cm^{-1} for LRRK2 Roc-COR, [Y1699C]LRRK2 Roc-COR and Rac1, respectively.

GTPase activity assays

GTP hydrolysis catalyzed by purified LRRK2 Roc-COR and its mutants was measured by the release of radio-labelled inorganic phosphate from [γ-^{32}P]GTP as described previously by us and Foulkes, *et al.* to monitor tyrosine phosphatase activity (Foulkes *et al.* 1981, Chia *et al.* 2010). In brief, the purified enzymes diluted to the designated concentrations were incubated at 30 ^{o}C with 30 mM Tris, pH 8.0, 1 mM $MgCl_2$ and 100 nM [γ-^{32}P]-GTP (specific radioactivity: ~5000 cpm/pmol) in a final volume of 25 µl for the indicated time periods. The GTP hydrolysis reaction was stopped by addition of 50 µl of a mixture consisting of 1.25 mM KH_2PO_4 and 0.5 M H_2SO_4. Released [^{32}P]inorganic phosphate was complexed with 100 µl of 5 % (w/v) ammonium molybdate. The phosphate-molybdate complex was extracted by the addition of 200 µl mixture of isobutanol and toluene mixed at a ratio of 1:1 (v/v). The mixtures were

centrifuged at 9,450 × g for 1 min to separate the aqueous and organic phase; 150 µl of the upper organic phase containing the molybdate-bound phosphate was taken out and mixed with scintillant (Ultima Gold XR, Packard Bioscience) prior to scintillation counting. The specific enzymatic activities of LRRK2 Roc-COR, [Y1699C]LRRK2 Roc-COR, and Rac1 were determined from the radioactivity associated with the organic phase. For the "blank" reaction of the assay, the aliquot of the diluted enzyme was replaced by an aliquot of the elution buffer of a similar volume.

Metabolic labeling of baculovirus-infected *Sf9* and *Sf21* cells with [^{32}P] inorganic phosphate

Both *Sf*9 and *Sf*21 cells infected with the baculovirus directing expression of LRRK2 Roc-COR were metabolically labelled with [^{32}P] inorganic phosphate. For labelling of *Sf*9 cells, cells were grown in a six-well plate (1×10^6 cells/well) in 3 ml of complete Grace's media and grown overnight at 25 ºC. They were then infected with baculovirus at MOI>1. At 24 h post infection, culture media were changed to 1 ml of fresh complete Grace's media with 0.25 mCi of [^{32}P] inorganic phosphate per well for metabolic labelling. At 48 h post infection, the cells were harvested and washed with incomplete Grace's media without fetal bovine serum. The harvested cells were re-suspended in 1 ml of Lysis Buffer and homogenized by repeated pipetting through a 200 µl pipette tip. After centrifugation, LRRK2 Roc-COR in the lysate was purified by binding to 500 µl of Ni^{2+}-NTA agarose. For labelling the *Sf*21 cells, 100 ml of cultured cells (2×10^6 cell per ml) were infected, metabolically labelled with 1 mCi of [^{32}P] inorganic phosphate at 24 h post infection. The labelled infected cells were harvested at 48 h post infection. Recombinant LRRK2 Roc-COR in the lysate was purified by incubation with 0.5 ml of Ni^{2+}-NTA agarose. After washing with Column Buffer, the LRRK2 Roc-COR-bound Ni^{2+}-NTA agarose was divided into two portions. For the first portion, the bound protein was eluted by incubation with 250 mM imidazole in Column Buffer. The eluted proteins were analyzed by SDS PAGE. An aliquot from each column fraction (5 µl out of a final volume of 100 µl) was spotted onto a 3MM filter paper. The radioactivity associated with each fraction was recorded by autoradiography. For the second portion, the suspension of LRRK2 Roc-COR-bound Ni^{2+}-NTA agarose was heat-

treated at ~95 ^{o}C for 5 min. After centrifugation, the supernatant contained the radioactively labelled compound(s) released from LRRK2 Roc-COR immobilized to Ni^{2+}-NTA agarose.

For thin layer chromatography (TLC) analysis, an aliquot of the supernatant was spotted onto a PEI Cellulose F TLC plate, and chromatographed for 1.5 h in 1 M KH_2PO_4, pH 3.4. Unlabeled GDP and GTP standards (30 nmol each) were included as controls. After chromatography, migration of the GTP and GDP standards was visualized by illumination with UV light. The [^{32}P] inorganic phosphate was detected by exposure to a phosphor-screen and imaged on a Typhoon phosphoimager at 200 nm per pixel. Identities of the radioactively labelled compounds co-purified with LRRK2 Roc-COR were determined by their co-migration with the standards.

Determination of metal ions in the purified LRRK2 Roc-COR preparations by inductively coupled plasma mass spectrometry (ICP-MS) and atomic emission spectroscopy (ICP-AES)

To prepare the samples for ICP-MS analysis, LRRK2 Roc-COR and [Y1699C]LRRK2 Roc-COR preparations expressed in *Sf*21 cells cultured in the serum-free medium were purified by Ni^{2+}-NTA agarose. The purified samples were dialyzed against the 4 × 1 l of Dialysis Buffer (20 mM Tris, 150 mM NaCl, 10 % (v/v) glycerol, pH 8.0). The dialyzed protein samples (at concentrations ranging from 6.6 – 12.5 µM) were used for analysis by ICP-MS. To prepare for ICP-MS, the diluted samples were further diluted 1/5 with 1 % (v/v) nitric acid in triplicate. Measurements were made using an Agilent 7700 series ICP-MS instrument under routine multi-element operating conditions using a Helium Reaction Gas Cell. The instrument was calibrated using 0, 5, 10, 50, 100 and 500 parts per billion (ppb) of certified multi-element ICP-MS standard calibration solutions (ICP-MS-CAL2-1, ICP-MS-CAL-3 and ICP-MS-CAL-4, Accustandard) for a range of elements. A certified internal standard solution containing 200 ppb of Yttrium (Y89) was used as an internal control (ICP-MS-IS-MIX1-1, Accustandard). After correcting for the raw ppb values of the buffer only, concentrations of Mg^{2+} bound to the recombinant LRRK2 Roc-COR and [Y1699C]LRRK2 Roc-COR

are expressed as µmol/l by calculation of the signals (in raw ppb values) as described in Supplemental Table S1.

To prepare the protein sample for ICP-AES analysis, LRRK2 Roc-COR expressed in *Sf*9 cells cultured in Grace's complete media was purified by Ni^{2+}-NTA column chromatography. After dialysis against 30 mM Tris, 150 mM NaCl, 0.1 mg/ml PMSF, pH 8.0, the purified protein sample (30 µg) was diluted to a final concentration of 0.01 mg/ml in 0.25 % (v/v) HNO_3 and 8 g/l CsCl (to suppress ionization of Na, K, Ca and Mg), and with 1 mg/l Rh and 1 mg/l Rb as internal standards to monitor ionization. The diluted LRRK2 Roc-COR protein samples were analyzed alone, and with addition of standards containing the indicated elements at 1, 0.1 and 0.01 mg/l, using a Vista AX CCD simultaneous ICP atomic emission spectrometer (Varian). Briefly, the sample was atomized in a nebulizer and injected directly into inductively-coupled plasma (Argon gas, 6000 to 8000 K). Light resulting from atomic emission was diffracted by an echelle grating and detected by a charged-couple device (CCD) camera. Atomic emission spectra were recorded, and intensities at the indicated wavelengths for each element were analyzed by comparing the LRRK2 Roc-COR samples alone with separate samples to which standards of known concentrations had been added. Sample intensity was subtracted from intensities of the standards, and a linear regression was performed. This allows the conversion of the measured intensity to the concentration of each element. Measured intensities for each element in the LRRK2 Roc-COR sample and in the buffer only sample were converted to concentration in mg/l. The concentration of Mg^{2+} co-purified with LRRK2 Roc-COR was determined by subtracting the concentration of Mg^{2+} in the buffer only sample from that in the LRRK2 Roc-COR sample.

Statistical analyses

No randomization or blinding was performed in this study. Assays of the GTPase activities of all recombinant proteins were conducted by more than one of the authors. All GTPase assays and the ICP-MS experiments were performed at least twice and with triplicate samples. More than five enzyme preparations of LRRK2 Roc-COR and [Y1699C]LRRK2 Roc-COR were used to perform the assay. The enzymatic activities of

LRRK2 Roc-COR and its mutants were presented as the mean ± SD. All statistical analyses of GTPase activity assay data were performed with student t-test and the Graphpad Prism software Version 7. All data points were included in the results presented. Thus, we did not conduct a test for outliers on the data.

RESULTS

Design of LRRK2 constructs to optimize expression of recombinant LRRK2 Roc-COR tandem domain

The functions of the two catalytic domains of LRRK2 have so far been explored using full-length LRRK2 immunoprecipitated from mammalian cells, two recombinant proteins containing the isolated LRRK2 Roc domain produced in *E. coli* (Deng *et al.* 2008, Liao et al. 2014), a fragment containing the Roc, COR and kinase domains (Rudi *et al.* 2015) and a fragment comprising the LRR, Roc, COR, kinase and WD40 domains (Anand *et al.* 2009). In order to further elucidate the function of the COR domain and assess the effects of the PD-causative Y1699C mutation mapped to the COR domain, a LRRK2 construct and its mutants consisting of the Roc and COR domains were produced for biochemical characterizations

We defined the LRRK2 Roc and COR domains to reside in the segment containing residues 1331-1840 of the human LRRK2 sequence with the aid of (i) alignment of Roco family members from diverse species (Bosgraaf & Van Haastert 2003, Civiero et al. 2012, Sejwal et al. 2017) and (ii) alignment of the LRRK2 sequence with sequences of Ras and the Roc-COR tandem domain of two prokaryotic Roco proteins with known three-dimensional structures (Gotthardt et al. 2008, Terheyden et al. 2015, Mills *et al.* 2012, Mills et al. 2014) (Supplemental Figure S1). The N-terminal truncation site (residue 1314) was chosen to include a loosely-conserved region of 27 residues N-terminal of the Roc domain P-loop; this region was predicted to be a linker between the LRR and Roc domains (Supplemental Figure S1). Truncation at this distance from the P-loop matches many structurally-stable truncations of Ras-like GTPases, and therefore was expected to minimize the impact of the truncation on the structure of the Roc domain. Determination of the truncation site at the C-terminus, on the other hand, presented a more difficult undertaking, as this region exhibits low sequence similarity to

the successfully-expressed and folded recombinant *C. tepidum* and *M. barkeri* Roco proteins, with potentially unpredictable effects on structure. Thus, we decided to include most of the putative linker connecting the COR domain to the kinase domain, in order to minimize the impact of truncation on the structural integrity of the COR domain. The chosen C-terminal truncation site (residue 1878) is 7 residues N-terminal to the glycine-rich loop of the kinase domain. The resultant construct consisting of residues 1314-1878 of the LRRK2 sequence, was used to generate three recombinant LRRK2 GTPase proteins expressed in *E. coli* and in baculovirus-infected insect cells (Figure 1). To facilitate their purification and detection, a poly-histidine (His_6) tag was added at the C-terminal end and a Flag or a GST-tag at the N-terminus of the recombinant proteins. Their expression levels and purities after affinity column chromatography were assessed. As listed in Figure 1, expression levels of GST-LRRK2 (1314-1878) in *E. coli* and baculovirus-infected *Sf*9 cells were low and the protein preparations after GSH-affinity column chromatography still contained several major protein contaminants (data not shown). In contrast, the Flag-LRRK2 (1314-1878) was expressed at a much higher level in baculovirus-infected insect cells. Furthermore, it could readily be purified by Ni^{2+}-NTA affinity column chromatography (Figure 2A). This recombinant LRRK2 fragment, which was used in biochemical analyses described in this manuscript, is referred to as LRRK2 Roc-COR.

To ascertain the impact of deletion of part of the linker connecting the LRR and Roc domains and that connecting the COR and kinase domains on the expression of LRRK2 GTPase, we generated the baculovirus directing expression of a shorter fragment (residues #1324-1858) of LRRK2. This shorter version of LRRK2 Roc-COR, referred to as short LRRK2 Roc-COR, consists of the intact Roc and COR domains as well as the truncated linkers at both the N-terminal and C-terminal ends (Figure 1). We found that short LRRK2 Roc-COR was expressed in insect cells at a level much lower than that of LRRK2 Roc-COR. Furthermore, a number of major protein contaminants were co-purified with short LRRK2 Roc-COR (Supplemental Figure S2). Taken together, our results suggest that the linker of LRR and Roc domains and/or that of the COR and Kinase domains stabilize LRRK2 GTPase and enhance its expression in insect cells. Of relevance, MASL1, the smallest human Roco protein, contains just the Roc-COR domain

flanked by a long N-terminal segment (residues 1-406) and a short C-terminal segment (residues 1029-1052 (Supplemental Figure S3). Similar to the role of the linker of the LRR and Roc domains and that of the COR and kinase domains of LRRK2, the N- and C-terminal segments may stabilize the structure of the MASL1 Roc-COR domain.

LRRK2 Roc-COR is folded, and migrates as a dimer in solution

LRRK2 Roc-COR was expressed at relatively high level [~ 10 mg/l of *Sf*21 cell culture (cell density: 2.0 - 2.5×10^6 cells/ml)] and purified to over 90% purity by Ni^{2+}-NTA affinity column chromatography (Figure 2). Its authenticity was confirmed by LC-MS/MS analysis of its tryptic fragments (Supplemental Figure S4). Circular dichroism analysis of its secondary structure contents revealed that it is folded (Figure 2B). The theoretical molecular mass of monomeric LRRK2 Roc-COR is 67 kDa. From the mobility of LRRK2 Roc-COR relative to those of the molecular size standards in the size exclusion column chromatography (Figure 2C and 2D), we determined the molecular mass of LRRK2 Roc-COR to be 111 kDa. The deviation of this value from that of the theoretical molecular mass (134 kDa) LRRK2 Roc-COR dimer suggests two possibilities. First, LRRK2 Roc-COR exists as a dimer in solution, and the deviation is a result of the low resolution of size exclusion column chromatography method. Second, LRRK2 Roc-COR exits a monomer with unique molecular shape such that it eluted from the size exclusion column with a molecular mass (111 kDa) significantly higher than the theoretical molecular mass (67 kDa) of the LRRK2 Roc-COR monomer.

The crystal structures of the two prokaryotic Roc-COR domains reveal that determinants governing their dimerization mainly reside in the C-terminal portion of the COR domain (Terheyden et al. 2015, Gotthardt et al. 2008). A truncation mutant of *M. barkeri* Roc-COR (Roc-CORΔC) lacking this portion of the COR domain existed as a monomer in solution, and exhibited much lower GTPase activity than that of wild type Roc-COR (Terheyden et al. 2015). We therefore attempted the same approach to explore whether the C-terminal portion of the COR domain mediates dimerization of LRRK2 Roc-COR, and whether dimerization enhances its GTPase activity. The C-terminal portion of LRRK2 COR domain was predicted to encompass residues 1674-1840 by alignment of the sequences of LRRK2, *C. tepidum* Roco and *M barkeri* Roco

(Supplemental Figure S1) and by inspecting the structure of *C. tepidum* Roco Figure 3A). Based upon this prediction, we design and generated the recombinant LRRK2 Roc-CORΔC encompassing residues 1314 to 1673 of human LRRK2, flanked by an N-terminal Flag tag and a C-terminal poly-His tag (Figures 1B and 3B). We were able to purify the recombinant LRRK2 Roc-CORΔC from the lysate of the infected *Sf*21 cells using Ni^{2+}-NTA affinity column chromatography (Supplemental Figure S5). However, the purified LRRK2 Roc-CORΔC readily aggregated to form precipitates in solution. In spite of this property, we managed to use the soluble recombinant LRRK2 Roc-CORΔC to determine its molecular mass by size exclusion chromatography. Figure 1E shows that it migrated as a protein of ~43 kDa (theoretical monomeric molecular mass: 43.7 kDa) in the chromatographic run (Figure 3C and 3D), suggesting that it exists as a monomer in solution.

Taken together, our data suggest that LRRK2 Roc-COR forms homodimers in solution, and the C-terminal portion of the COR domain governs its dimerization.

Mg^{2+} and guanine nucleotides co-purified with LRRK2 Roc-COR

Whether the enzymatic properties of LRRK2 Roc-COR domains match more closely with those of the conventional Ras-like GTPases or with those of the numerous emerging examples of GADs, is an outstanding question in the field of LRRK2 research. To address this question, we attempted to measure the affinity of the LRRK2 Roc-COR for two fluorescent GTP analogs: 2'-(or-3')-O-(N-methylanthraniloyl)-GTP (mant-GTP) and its non-hydrolyzable analog mant-GMPPNP. However, we failed to detect significant binding of mant-GTP or mant-GMPPNP to LRRK2 Roc-COR (data not shown). One potential explanation for this observation is that unlike the LRRK2 Roc domain, which binds guanine nucleotides with relatively low affinity (Liao et al. 2014), LRRK2 Roc-COR binds guanine nucleotides tightly. As such, most of the recombinant LRRK2 Roc-COR molecules used in our analysis may have already had a co-purified Mg^{2+}-GTP or Mg^{2+}-GDP tightly bound to their active site. Consequently, they were unable to exchange the bound Mg^{2+}-GTP and Mg^{2+}-GDP for the exogenous mant-GTP and mant-GMPPNP under the conditions we conducted the analysis. In agreement with this explanation, the UV absorption spectrum of the purified LRRK2 Roc-COR preparation revealed

significant absorption at 260 nm, suggesting the presence of UV-absorbing materials co-purified with LRRK2 Roc-COR (Figure 4A). The likely candidates of the UV-absorbing material at 260 nm are guanine nucleotides. Relevant to this, Poe, *et al*. reported that recombinant viral K-Ras with GDP bound to its active site at 1:1 stoichiometry also gave a UV-visible absorption spectrum with significant UV absorption at 260 nm (Poe *et al.* 1985). Thus, these findings suggest that significant UV absorption at 260 nm found in the UV-visible absorption spectra of LRRK2 Roc-COR (Figure 4A) is caused by the guanine nucleotides tightly bound to their active sites.

To confirm that LRRK2 Roc-COR is capable of tight binding to guanine nucleotides in cells, and to determine whether the GTP- or GDP- bound form predominates, bound nucleotides were examined in LRRK2 Roc-COR purified from infected *Sf*9 and *Sf*21 cells metabolically labelled with ^{32}P-inorganic phosphate. As shown in Figure 4C and Supplemental Figure S6, LRRK2 Roc-COR was co-purified with a radioactive compound. This tightly bound radioactive compound dissociated from LRRK2 Roc-COR upon heat treatment of the purified protein preparations. TLC of the released radioactive compound with GTP and GDP standards shows that GTP was the guanine nucleotide co-purified with LRRK2 Roc-COR expressed in *Sf*21 cells cultured in serum-free media (Figure 4C). Interestingly, GDP was the radioactive compound co-purified with LRRK2 Roc-COR expressed in *Sf*9 cells cultured in Graces' media supplemented with 10% fetal bovine serum (Supplemental Figure S6C). The predominance of GTP bound to LRRK2 Roc-COR expressed in *Sf*21 cells cultured in serum-free media (Figure 4) suggests that the GTPase activity of recombinant LRRK2 Roc-COR was suppressed in these cells. In contrast, LRRK2 Roc-COR expressed in *Sf*9 cells cultured in Graces' medium with fetal bovine serum was more catalytically active and capable of hydrolyzing all the bound GTP to GDP (Supplemental Figure S6). Why LRRK2 Roc-COR proteins expressed in different types of insect cells and/or cultured in different media exhibit different catalytic activity in cells remains unclear. Nevertheless, our data suggest that similar to the conventional Ras-like GTPases, LRRK2 Roc-COR binds both GTP and GDP with very high affinities.

GTPases bind guanine nucleotides complexed with a Mg^{2+} ion as a cofactor. To further confirm tight binding of LRRK2 Roc-COR to Mg^{2+}-GTP or Mg^{2+}-GDP, purified

LRRK2 Roc-COR samples expressed in *Sf*21 cells were analyzed for the bound metals using inductively coupled plasma mass spectrometry (ICP-MS). The concentrations of Mg^{2+} detected in the purified preparations of LRRK2 Roc-COR were determined from the raw ppb values (Supplemental Table S1). From these concentrations, the stoichiometry of Mg^{2+} co-purified with LRRK2 Roc-COR determined in the three replicates ranges from 0.8 - 1.0 mol/mol of protein (Figure 5A). In addition to ICP-MS, ICP-AES was also used to measure the magnesium ions co-purified with LRRK2 Roc-COR expressed in *Sf*9 cells (Figure 5B). Our measurement also reveals a stoichiometry of ~1.0 mol. of Mg^{2+} per mol of LRRK2 Roc-COR.

Thr-1348 of LRRK2 corresponds to the conserved active site threonine residue critical to binding of guanine nucleotides in GTPases (Figure S1). Its mutation is predicted to abolish the GTP-binding ability and GTPase activity of LRRK2-Roc-COR. We therefore generated the [T1348N]LRRK2 Roc-COR mutant to investigate if Mg^{2+} and GTP (Figures 3C and 4) co-purified with LRRK2 Roc-COR were stoichiometrically bound to its active site. Similar to the effect of the T1348N mutation on the GTPase activity of full-length recombinant LRRK2 (Ito *et al.* 2007, Biosa *et al.* 2013), this mutation completely abolished the GTPase activity LRRK2 Roc-COR (Supplemental Figure S7). Additionally, this mutation significantly reduced the expression level of the LRRK2 Roc-COR mutant (data not shown). The low yield of this mutant recombinant protein preparation prevented us from carrying out the ICP-MS or ICP-AES experiments to ascertain if this mutation abolishes the ability of LRRK2 Roc-COR to bind Mg^{2+} and guanine nucleotides.

In summary, the consistent presence of Mg^{2+} at close to 1:1 stoichiometry in the LRRK2 Roc-COR preparations determined by both ICP-MS and ICP-AES (Figure 4) and the demonstration of tight binding of guanine nucleotides to LRRK2 Roc-COR (Figure 3 and Supplemental Figure S6), suggest that LRRK2 Roc-COR contains Mg^{2+}-GTP or Mg^{2+}-GDP bound to its active site at close to 1:1 stoichiometry.

It took us ~6 h to purify the recombinant LRRK2 Roc-COR from the *Sf*21 cells metabolically labelled with [^{32}P]-inorganic phosphate. In spite of such a long period of purification, we did not detect a significant amount of radioactive GDP in the guanine nucleotide co-purified with LRRK2 Roc-COR. Instead, GTP was the only detectable

guanine nucleotide co-purified with LRRK2 Roc-COR (Figure 4C). This results suggest that the intrinsic GTPase activity of LRRK2 Roc-COR is so low that we were unable to detect the GDP generated as a result of hydrolysis of the tightly bound GTP.

LRRK2 Roc-COR exhibits weak GTPase activity with a nanomolar K_m value

Although our data shown in Figures 4 and 5 indicate that the majority of the purified LRRK2 Roc-COR protein molecules were tightly bound to Mg^{2+}-GTP, the purified LRRK2 Roc-COR preparation still exhibited weak GTPase activity (Figure 6A). Furthermore, this weak activity is abolished when Thr-1348 critical to binding of guanine nucleotides is mutated to Asn (Supplemental Figure S7). We first compared the specific enzymatic activity of LRRK2 Roc-COR with that of a conventional Ras-like GTPase Rac1. Our analysis revealed that the specific enzymatic activity of LRRK2 Roc-COR is almost as low as that of Rac1 under the conditions we performed the assay (Figure 6B). Thus, similar to Rac1, the weak GTPase activity of LRRK2 Roc-COR is likely caused by the slow exchange of the bound guanine nucleotide with exogenous [γ-^{32}P]GTP as well as the low intrinsic efficiencies of its active site in catalyzing hydrolysis of the bound GTP.

To define the enzymatic properties of LRRK2 Roc-COR, we performed kinetic analysis of its GTPase activity. Figure 6C shows that LRRK2 Roc-COR catalyzed GTP hydrolysis with K_m of 22 nM. The nanomolar K_m value is in agreement with our findings presented in Figures 3 and 4, which suggest that LRRK2 Roc-COR binds Mg^{2+}-GDP/GTP tightly. The tight binding limits turnover of guanine nucleotides in the catalytic cycle of GTP hydrolysis catalyzed by LRRK2 Roc-COR, accounting for the very low k_{cat} value (0.47×10^{-3} min^{-1}) of its GTPase activity. From this k_{cat} value, we calculated the turnover time for the hydrolysis of one molecule of GTP by each molecule of LRRK2 Roc-COR to be 2127.65 min (~35.5 h). Such a long turnover time explains why we failed to detect GDP as a guanine nucleotide co-purified with LRRK2 Roc-COR from the infected *Sf*21 cells metabolically labelled with [^{32}P]-inorganic phosphate (Figure 4C) – the turnover time is significantly longer than the duration (6 h) we took to isolate LRRK2 Roc-COR prior to releasing the bound guanine nucleotide for TLC analysis.

Several groups of researchers have performed kinetic analysis of the GTPase activity of full-length LRRK2 and two truncated LRRK2 fragments (i) LRRK2(Roc-COR/kinase) consisting of the Roc-COR and kinase domains and (ii) LRRK2(LRR-WD) containing LRR, Roc-COR, kinase and WD40 domains (Table 1) (Liu *et al.* 2010, Rudi et al. 2015, Liu *et al.* 2012). These researchers separately revealed that full-length LRRK2 and truncated LRRK2 mutants with both intact Roc-COR and kinase domains catalyzed GTP hydrolysis with K_m values (210 μM – 700 μM) much higher than that of LRRK2 Roc-COR, and with k_{cat} values much higher than that of LRRK2 Roc-COR (Table 1). These results suggest that the presence of kinase domain and other functional domains somehow reduces the affinity of the Roc-COR domain for guanine nucleotides; the lower affinity likely allows a higher turnover rate of guanine nucleotides in catalysis. Hence, full-length LRRK2 and LRRK2 fragments consisting of intact Roc-COR, kinase domains and other functional domains are predicted to hydrolyze GTP with catalytic efficiencies higher than that of LRRK2 Roc-COR. In agreement with this prediction, we found that the specific enzymatic activities of LRRK2(LRR-WD) and its G2019S mutant are ~8 to 10-fold higher than that of LRRK2 RocCOR (Table 1, Supplemental Figure S8).

Taken together, our data shown in Figures 4, 5 and 6C indicate that similar to the conventional Ras-like GTPases, LRRK2 Roc-COR in isolation binds guanine nucleotides with high affinities and catalyzes GTP hydrolysis with a very low efficiency. Results shown in Table 1 and Supplemental Figure S8 suggest that in the presence of other functional domains, LRRK2 GTPase domain catalyzes GTP hydrolysis with a higher K_m and a higher k_{cat}

The PD-causative Y1699C mutation does not perturb the secondary structural contents, guanine nucleotide-binding capacity and catalytic activity of LRRK2 Roc-COR

We generated the [Y1699C]LRRK2 Roc-COR to examine how the PD-causative Y1699C mutation impacts on the secondary structure contents, guanine nucleotide-binding capacity and GTPase activity of LRRK2 Roc-COR. Supplemental Figure S9 shows that [Y1699C]LRRK2 Roc-COR was expressed at a relatively high level and purified to a similar purity as the wild type LRRK2 Roc-COR protein. Tyr-1699 was predicted to reside at the interface between the Roc and COR domains. Thus, Y1699C

mutation can potentially perturb the interactions between the two domains, and this in turn can potentially impact the GTPase activity and stability of LRRK2 Roc-COR domain (Mills et al. 2014) (Daniels *et al.* 2011, Li *et al.* 2007, Lewis *et al.* 2007, Guo *et al.* 2007).

The CD spectra of wild type LRRK2 Roc-COR and [Y1699C] LRRK2 Roc-COR (Figure 6D) indicate that the mutation induces minor perturbations to the secondary structure contents of LRRK2 tandem Roc-COR domain – a slight decrease on the α-helical structure contents and a slight increase in β-strand contents. We then examined how the secondary structure contents of LRRK2 Roc-COR and [Y1699C]LRRK2 Roc-COR are perturbed by increasing concentrations of guanidine hydrochloride. Figure 6E shows that the Y1699C mutation did not significantly alter the sensitivity of the LRRK2 Roc-COR protein to structural perturbation by the denaturant, suggesting that the mutation does not significantly affect the stability of LRRK2 Roc-COR in solution.

To ascertain how the Y1699C mutation impacts the capacity of LRRK2 Roc-COR to bind guanine nucleotides, we compared the UV absorption spectra of the purified preparations of wild type and [Y1699C]LRRK2 Roc-COR. Both spectra shown in Figure 4A exhibit significant absorption at 260 nm, suggesting tight binding of guanine nucleotide to the active site of [Y1699C]LRRK2 Roc-COR, similar to wild-type. Indeed, ICP-MS analysis revealed that an approximately 1:1 stoichiometry of Mg^{2+} ion bound to [Y1699C]LRRK2 Roc-COR (Figure 5A). Thus, the Y1699C mutation does not affect the ability of LRRK2 Roc-COR to tightly bind guanine nucleotide.

In contrast to the observations made by Daniels *et al.* that the Y1699C mutation almost completely abolished the GTPase activity of full-length LRRK2 (Daniels et al. 2011), we found that the mutation did not significantly affect the GTPase activity of LRRK2 Roc-COR (Figure 6A).

Taken together, our results shown in Figures 3, 4 and 5 indicate that the PD-causative Y1699C mutation does not significantly alter the secondary structure contents and does not negatively impact the stability, GTP-binding capacity and catalytic activity of LRRK2 Roc-COR tandem domain.

DISCUSSION

Our results reveal that similar to the GADs of known structures (Terheyden et al. 2015, Gotthardt et al. 2008), the C-terminal subdomain of COR domain of LRRK2 contains determinants mediating homo-dimerization. In spite of the structural similarities to GADs, LRRK2 Roc-COR exhibits enzymatic properties similar to those of Ras-like GTPases. like Ras-like GTPases, LRRK2 Roc-COR binds Mg^{2+}-GDP or Mg^{2+}-GTP tightly at stoichiometry approaching 1 mol of Mg^{2+}-GDP/GTP per mol of LRRK2 Roc-COR protein. Furthermore, similar to the Ras superfamily of GTPases, LRRK2 Roc-COR exhibits very low GTPase activity. Collectively, these results suggest that LRRK2 Roc-COR functions as a conventional Ras-like GTPase. Presumably, it requires the assistance of GEF(s) and GAP(s) to facilitate exchange of the guanine nucleotide tightly bound to its active site, and to enhance its catalysis of hydrolysis of GTP to GDP, respectively. We also generated the [Y1699C]LRRK2 Roc-COR and used it to demonstrate that the PD-associated Y1699C mutation does not significantly impact the secondary structure contents, stability, guanine nucleotide-binding capacity and GTPase activity of the LRRK2 Roc-COR tandem domain in isolation. Of relevance, the same mutation reduces the rate of GTP hydrolysis catalyzed by full-length LRRK2 *in vitro* (Daniels et al. 2011). Thus, the Y1699C mutation reduces the GTPase activity of LRRK2 only when the Roc-COR tandem domain is interacting with other functional domains. Since ours is the first study of the biochemical properties of the isolated LRRK2 Roc-COR tandem domain, our findings raise a number of questions related to the structure and regulation of LRRK2. These questions are discussed below.

Other evidence suggesting LRRK2 as a conventional Ras-like GTPase

The two prokaryotic Roc-COR domains with known three-dimensional structures form dimers and contain a conserved arginine that acts as an “arginine finger” inserting into the active site of the neighboring Roc-COR monomer. This arginine residue is predicted to participate in catalysis *in trans* by stabilizing the transition-state intermediate of GTP hydrolysis. Mutations perturbing or abolishing dimerization cause significant reduction in GTPase activity (Gotthardt et al. 2008, Terheyden et al. 2015). Besides, mutation of the putative “arginine finger” residue either completely abolished or

significantly reduced the catalytic activity of the *C. tepidum* and *M. Barkeri* Roco proteins, further confirming that dimerization and insertion of the arginine finger *in trans* to the Roc domain active site is critical for catalysis (Gotthardt et al. 2008, Terheyden et al. 2015). Furthermore, the two prokaryotic Roco proteins bind GDP and GTP analogs with affinities (K_D values in the μM range) much lower than those of the Ras-like GTPases (K_D values in the nM range), suggesting that they do not require GEFs for the exchange of guanine nucleotides in their active sites. These results indicate that the two prokaryotic Roc-COR domains are GADs and the conserved arginine finger governs activation of their GTPase activity upon dimerization.

However, this arginine residue is missing in the Roc-COR domain of LRRK2, (Gotthardt et al. 2008) (Supplemental Figure S1), prompting some researchers to suggest that LRRK2 is not a GAD (Liao et al. 2014). In agreement with this prediction, Liao *et al.* demonstrated that LRRK2 Roc domain monomer is catalytically active, suggesting that dimerization is not necessary for the LRRK2 Roc domain GTPase activity (Liao et al. 2014). Recently, Deyaert, *et al.* reported that *C. tepidum* Roc-COR, which is a *bona fide* GAD, undergoes a monomer-dimer transition during GTP turnover *in vitro* (Deyaert et al. 2017). Unlike *C tepidum* Roc-COR, full-length LRRK2 forms dimers regardless of whether Mg^{2+}-GDP or Mg^{2+}-GTP analog resides in the Roc domain active site (Taymans *et al.* 2011). Thus, these findings together further support that LRRK2 Roc-COR exhibits enzymatic properties similar to those of conventional Ras-like GTPases. In spite of such a similarity, LRRK2 Roc-COR is not a *bona fide* Ras-like GTPase because of its GAD-like ability to form homodimers via the C-terminal portion of its COR domain. For this reason, LRRK2 Roc-COR can be considered as a GAD-like GTPase exhibiting Ras-like GTPase enzymatic properties.

Is it possible to measure the rate of guanine nucleotide exchange of LRRK2 Roc-COR in vitro?

The low K_M value (22 nM) of the GTP hydrolysis reaction catalyzed by LRRK2 Roc-COR suggests that it binds GTP with a high affinity. However, K_M is not a true measure of the affinity of LRRK2 Roc-COR for GTP. We therefore attempted to determine the dissociation constant of binding of radioactive GTP to LRRK2 Roc-COR

as a direct measure of the affinity of LRRK2 Roc-COR for GTP. In brief, we incubated LRRK2 Roc-COR with [γ-^{32}P]GTP for 1-2 h; this is followed by immunoprecipitation of LRRK2 Roc-COR with the anti-Flag antibody-agarose to separate the [γ-^{32}P]GTP complexed with LRRK2 Roc-COR from the unbound [γ-^{32}P]GTP. Since the incubation period (1-2 h) is much shorter than the turnover time (~35.5 h) of GTP hydrolysis catalyzed by LRRK2 Roc-COR, we predict that GTP bound to the active site of LRRK2 Roc-COR remains intact regardless of whether the radioactive ^{32}P-phosphate group is at the α-, β- or γ-position. However, we failed to detect significantly binding of [γ-^{32}P]GTP to LRRK2 Roc-COR, suggesting that the exchange of the GTP bound to LRRK2 Roc-COR for the exogenous [γ-^{32}P]GTP occurred at a rate that is not detectable by this method.

Since LRRK2 Roc-COR binds guanine nucleotides tightly, it likely requires a guanine nucleotide exchange factor (GEF) to enhance the release of the tightly bound guanine nucleotide in exchange for the exogenous GTP or GDP. Direct measurement of the dissociation constants of LRRK2 Roc-COR for GTP and GDP using our method awaits the discovery of the LRRK2 GEF.

How does Y1699C mutation impact on the structure and function of LRRK2?

Based upon the three-dimensional structure of the Roc-COR domain of *C. tepidum* Roc-COR protein, Gotthardt, et al. mapped LRRK2 Tyr-1699 to the interface between the Roc and COR domains (Figure 3A) (Gotthardt et al. 2008). They then reported that mutation of Tyr-804 in *C. tepidum* Roc-COR, predicted as a homologous residue to human LRRK2 Tyr-1699 by sequence alignment, led to an eight-fold reduction of GTPase activity. Presumably, this mutation perturbs the Roc/COR interface and in turn adversely affects the catalytic activity (Gotthardt et al. 2008). Based upon this result, Y1699C mutation is expected to perturb the LRRK2 Roc-COR structure and in turn reduce its catalytic activity. In contrast to this prediction, we found that Y1699C mutation did not significantly impact on the secondary structure contents, stability and catalytic activity of LRRK2 Roc-COR (Figure 6).

Several groups of researchers investigated the impact of Y1699C mutation on the GTPase activity of recombinant full length LRRK2. Unlike the lack of effect on the

GTPase activity of LRRK2 Roc-COR protein (Figure 6), the mutation significantly reduced the GTPase activity of full-length LRRK2 (Daniels et al. 2011, Xiong *et al.* 2010). The discrepancy of our results and the findings by Daniels *et al.* suggests that Y1699C mutation may indirectly alter the GTPase activity of the Roc domain by aberrant regulation of other functional domains in full-length LRRK2. Specifically, the Y1699C mutation leads to decreased phosphorylation of Ser-910, Ser-935, Ser-955 and Ser-973 in the ankyrin region, as well as changes in autophosphorylation levels at Thr-1357 in the Roc domain and at Ser-1292 in the LRR region in cells. Additionally, the Y1699C mutation abolishes LRRK2 binding to 14-3-3 in cells (Doggett *et al.* 2012, Li *et al.* 2011, Nichols *et al.* 2010, Henry *et al.* 2015, Kamikawaji *et al.* 2013). These changes may underpin the significant reduction in GTPase activity of full-length LRRK2 carrying the Y1699C mutation. Thus, rather than directly impacting the structure and stability of the LRRK2 Roc-COR domains, this mutation may affect the GTPase activity by perturbing interactions of the Roc-COR domains with other domains and/or autophosphorylation of LRRK2.

Implications of the differences in the enzymatic properties of the GTPase activity of LRRK2 Roc-COR and full-length LRRK2

Unlike LRRK2 Roc-COR, which binds guanine nucleotides with high affinities, full-length LRRK2 binds guanine nucleotides with a low affinity (0.36 μM) (Table 1) (Civiero et al. 2012). Furthermore, full-length LRRK2, the truncated LRRK2 fragments consisting of the Roc-COR domain and the kinase domain with and without the LRR and WD40 domains all exhibited catalytic properties significantly different from those of LRRK2 Roc-COR. They hydrolyze GTP with much higher catalytic activity (Supplemental Figure 8) and with K_m and k_{cat} values much higher than those of LRRK2 Roc-COR (Table 1). These findings suggest that interactions of the Roc-COR domain with other functional domains of LRRK2 perturb the structure of Roc-COR to lower its affinity for guanine nucleotides, and in turn increases its GTPase activity. Further investigation is needed to unveil how other functional domains interact with the Roc-COR tandem domain in intact LRRK2 to regulate the affinities for guanine nucleotides and catalysis of GTP hydrolysis.

How can future studies of LRRK2 Roc-COR bridge the knowledge gaps in the field of LRRK2 research?

The LRRK2 Roc-COR construct and its mutants described in this study open up opportunities for further studies to define the three-dimensional structure of the LRRK2 Roc-COR tandem domain and how the tandem domain interacts with other LRRK2 domains. Since LRRK2 Roc-COR exhibits a very low GTPase activity (Figure 6C and Supplemental Figure S8), it potentially requires GAPs to enhance the rate of GTP hydrolysis. Xiong, *et al.* discovered ArfGAP1 as a potential GAP of LRRK2 because it binds full-length LRRK2 and enhances LRRK2 GTPase activity by ~2.5-fold (Xiong *et al.* 2012). However, such a modest rate enhancement of LRRK2 GTPase activity by ArfGAP2 is much lower than that of Ras-GAPs, which can enhance Ras GTPase activity by ~10,000-fold *in vitro* (Shutes & Der 2006). These findings imply that GTPase-activator activity of ArfGAP1 needs to be significantly up-regulated for efficient regulation of LRRK2 GTPase activity. The recombinant LRRK2 Roc-COR complexed with [^{32}P]GTP described in this manuscript (Figure 3) can be exploited for the design of *in vitro* assays to further characterize how the GTPase activator activity of ArfGAP1 is regulated.

Identifying the downstream effectors of LRRK2 GTPase domains is another frontier in the field of LRRK2 research. The LRRK2 Roc-COR construct can be used in future investigations as a bait to search for the downstream effectors of LRRK2 GTPase domain.

Involves human subjects:
If yes: Informed consent & ethics approval achieved:
=> if yes, please ensure that the info "Informed consent was achieved for all subjects, and the experiments were approved by the local ethics committee." is included in the Methods.

ARRIVE guidelines have been followed:
No
=> if No or if it is a Review or Editorial, skip complete sentence => if Yes, insert "All experiments were conducted in compliance with the ARRIVE guidelines." unless it is a Review or Editorial

Conflicts of interest: None
=> if 'none', insert "The authors have no conflict of interest to declare."
=> otherwise insert info unless it is already included

Acknowledgements/Conflict of interest disclosure

We would like to thank Dr. Matthew Farrer of the University of British Columbia for providing us the pcDNA3-LRRK2 plasmid and Ms Irene Volitakis of the Florey Neuroscience Institute for her help in analyzing the metal ion contents of the purified LRRK2 Roc-COR and [Y1699C]LRRK2 Roc-COR preparations with ICP-MS. We are also grateful to the staff in the Australian Nuclear Science and Technology Organization (ANSTOS) in Lucas Height, New South Wales, for their help in ICP-AES analysis. The work reported in this manuscript was supported by a project grant (App#566743) from the National Health and Medical Research Council of Australia to H.-C.C. and J.G.C. R.D.M. was supported by an Australian Postgraduate Award, a Dowd Foundation Neuroscience Research Scholarship and an AINSE (Australian Institute of Nuclear Science and Engineering) Postgraduate Research Award.

We declare that there is no conflict of interest for the work presented in this manuscript.

Open Science Badges

This article has received a badge for *__Open Materials__* because it provided all relevant information to reproduce the study in the manuscript. The complete Open Science Disclosure form for this article can be found at the end of the article. More information

about the Open Practices badges can be found at https://cos.io/our-services/open-science-badges/.

List of abbreviation

ArfGAP1: ADP-ribosylation factor GTPase-activating protein 1

C. tepidum: *Chlorobium tepidum*

COR: C-terminal of Roc

GAP: GTPase-activating protein

GEF: Guanine nucleotide exchange factor

LRRK2: Leucine-rich repeat kinase 2

M. barkeri: *Methanosarcina barkeri*

Mant-GTP: 2' – (or-3' - O - (N' - Methylanthraniloyl)guanosine - 5' - O - triphosphate

Mant-GMPPNP: 2'-(or-3')-O-(N-Methylanthraniloyl)-β:γ-Imidoguanosine 5'-Triphosphate

Roco: A conserved supradomain that contains a Ras-like GTPase domain, called Roc, and a COR (C-terminal of Roc) domain.

Roc: Ras of complex

*Sf*21 cells: *Spodoptera frugiperda* Clone 21 cells

*Sf*9 cells: *Spodoptera frugiperda* Clone 9 cells

Roc-COR (This study)	22 nM (WT)	0.47×10^{-3} min^{-1}	Residues #1314 - 1878 Expressed in *Sf*21 insect cells Y1699C mutation has no effect on activity
Roc-COR/kinase (Rudi et al. 2015)	343 μM (WT) 541 μM (R1441C)	0.8 min^{-1} (WT) 0.37 min^{-1} (R1441C)	Residues #1334 - #2147 Expressed in *Sf*9 insect cells

Full-length (Civiero et al. 2012)	Apparent K_D 0.36 μM		Expressed in HEK293T
Full-length (Liu et al. 2010)	210 μM	13.8 min^{-1} (0.23 s^{-1})	Purified from murine brain
Roc (Liao et al. 2014)	553 μM (WT) 112 μM (R1441H)	0.020 min^{-1} (WT) 0.009 min^{-1} (R1441H)	Residues #1329-1520 Expressed in *E. coli* (exists as monomer).
Roc (Liu *et al.* 2016)	154 μM	0.007 min^{-1}	Residues #1333-1516 Expressed in *E. coli*
LRRK2 (LRR-WD) containing LRR/Roc-COR/kinase/WD40 (Liu et al. 2012)	700 μM (WT); 400 μM (G2019S)	2.4 min^{-1} (0.04 s^{-1}) (WT); 1.8 min^{-1} (0.03 s^{-1}) (G2019S)	Residues #970-2527 Expressed in baculovirus-infected insect cells (from Invitrogen/ThermoFisher)
LRRK2 (LRR-WD) and its G2019S mutant containing LRR/Roc-COR/kinase/WD40 (this study)	The specific activities of LRRK2 (LRR-WD) are much higher than that of LRRK2 Roc-COR. LRRK2(LRR-WD): $17.1\times10^{-3} \pm 7.9\times10^{-3}$ min^{-1} G2019SLRRK2(LRR-WD): $13.4\times10^{-3} \pm 7.0\times10^{-3}$ min^{-1}		Residues #970-2527 Expressed in baculovirus-infected insect cells (from Invitrogen)
	K_m	**k_{cat}**	
Apo-RhoA (Zhang *et al.* 2000)	3.01 μM	50.5 min^{-1}	The apo-enzymes without Mg^{2+}-GDP/GTP bound to the active site were used for the kinetic analysis.
Apo-Rac1 (Zhang et al. 2000)	4.48 μM	95.9 min^{-1}	
Apo-Cdc42 (Zhang et al. 2000)	3.40 μM	1380 min^{-1}	
Apo-Ras (Hall *et al.* 2002)	Not determined	0.012 min^{-1} (0.0002 s^{-1})	The apo-enzyme without Mg^{2+}-GDP/GTP bound to the active site was used for

			the kinetic analysis.

Table 1 Comparison of the kinetic parameters of GTPase activity of different constructs of LRRK2 with those of several Ras-like GTPases

Figure Legends

Figure 1 The seven recombinant LRRK2 protein constructs generated

A. Functional domains of LRRK2. B. A summary of expression systems, purities, yields and stabilities of the six recombinant protein constructs containing the LRRK2 Roc-COR domains and the linkers connecting the tandem domain to the LRR and kinase domains. The numbers in the second column indicate residue numbers of the human LRRK2 sequence.

Figure 2 Recombinant LRRK2 Roc-COR expressed in insect cells is folded and exists as dimers in solution

A. Protein profile of column fractions of Ni^{2+}-NTA affinity column chromatography of *Sf*21 cell lysates expressing LRRK2 Roc-COR. **B.** Secondary structure contents of purified LRRK2 Roc-COR determined by circular dichroism (CD) and analysis of the CD spectrum by the Bestsel structure prediction program. The table shows the secondary structure contents of LRRK2 Roc-COR determined from the spectrum. **C.** Purified recombinant LRRK2 Roc-COR in conjunction with different molecular mass protein standards were applied to a Superose-12 size exclusion column. The column fractions (0.25 ml per fraction) were analyzed by SDS-PAGE. Arrows on the right: mobilities of LRRK2 Roc-COR and the molecular mass protein standards. Arrows at the top: the peak column fractions of the molecular mass standards including apoferritin (443 kDa), β-amylase (200 kDa), alcohol dehydrogenase (150 kDa) and chymotrypsin (25 kDa). The peak column fraction of LRRK2 Roc-COR is marked by a red arrow. D. The plot of $\log_{10}$

molecular weight versus the ratio of the elution volume (V_e) to the column void volume (V_o) of all proteins to determine the molecular mass of LRRK2 Roc-COR in solution.

Figure 3 The truncated mutant LRRK2 Roc-CORΔC lacking the C-terminal subdomain of the COR domain elutes as a monomer in size exclusion column chromatography

A. A model of the Roc-COR domain of *C. tepidum* Roco protein generated from its three-dimensional structure. The Roc domain in monomer B was generated by docking the Roc domain structure of monomer A to the COR domain of monomer B. The C-terminal portion of the COR domain mediating homo-dimerization of the Roco protein. The Y804 residues homologous to the Y1699 of human LRRK2 in the two protomers are shown. Yellow ribbons: Roc domain of monomer A. Orange ribbons: Roc domain of monomer A docked to monomer B. Green ribbons: COR domain of monomer A. Blue ribbons: COR domain of monomer B. PDB ID: 3DPU. **B.** Schematic diagram depicting the boundaries of truncation and the affinity tags of LRRK2 Roc-COR and LRRK2 Roc-CORΔC. **C.** The purified LRRK2 Roc-CORΔC was prone to aggregation and precipitation during concentration by centrifugal filter units. An aliquot (4.5 ml) of the purified LRRK2 Roc-CORΔC of the Ni^{2+}-NTA column step without concentration was applied to a Superdex 200 Hiload 16/60 size exclusion column for chromatography. The column fractions (1 ml per fraction) were analyzed by SDS-PAGE. Proteins in the column fractions were detected by Coomassie blue staining (upper panel). LRRK2 Roc-CORΔC in the column fractions was detected by anti-Flag Western blot (lower panel). **D.** The Superdex 200 Hiload 16/60 size exclusion column was calibrated in a separate run with a number of molecular weight standards with molecular masses ranging from 25 kDa to 200 kDa. The plot of $\log_{10}$ molecular weight versus the ratio of the elution volume (V_e) to the column void volume (V_o) of the protein standards and LRRK2 Roc-CORΔC. From the plot, the molecular mass of LRRK2 Roc-COR in solution was calculated to be 43 kDa. The calculated molecular mass is in agreement with the theoretical monomer molecular mass of LRRK2 Roc-CORΔC (43.7 kDa).

Figure 4 Evidence demonstrating tight binding of guanine nucleotides to LRRK2 Roc-COR and its mutant

A. Absorption spectra of purified recombinant LRRK2 Roc-COR and [Y1699C]LRRK2 Roc-COR expressed in *Sf21* insect cells. The absorbance peaks at 260 nm and 280 nm are indicated by a blue arrow and a red arrow, respectively. **B.** Co-purification of non-covalently bound radioactive compound(s) with recombinant LRRK2 Roc-COR from the lysate of infected *Sf*21 cells metabolically with [^{32}P] inorganic phosphate. Upper panel: the elution profile of LRRK2 Roc-COR from Ni^{2+}-NTA column revealed by SDS-PAGE of proteins in the column fractions. Lower panel: the autoradiograph showing co-purification of radioactive compounds with LRRK2 Roc-COR. An aliquot from each of the corresponding fractions shown in the upper panel was spotted onto a filter paper. The radioactivity co-purified with LRRK2 Roc-COR in each fraction was detected by phosphoimaging and shown in the autoradiogram. **C.** Recombinant LRRK2 Roc-COR in the *Sf21* insect cell lysates was first bound to Ni^{2+}-NTA agarose. The immobilized LRRK2 Roc-COR was denatured by heat treatment at ~95 ^{o}C for 5 min. After centrifugation, the non-covalently bound radioactive compound(s) released from the denatured LRRK2 Roc-COR was mixed with GDP and GTP standards for analysis by TLC. Right panel: mobilities of GDP and GTP in the TLC plate revealed by UV light illumination. Left panel: the autoradiogram showing the mobilities of the radioactive compound(s) released from the denatured immobilized LRRK2 Roc-COR.

Figure 5 Measurement of magnesium ions in the purified preparations of LRRK2 Roc-COR and [Y1699C]LRRK2 Roc-COR by inductively coupled plasma-mass spectrometry (ICP-MS) and inductively coupled plasma-atomic emission spectroscopy (ICP-AES)

A. Recombinant LRRK2 Roc-COR and [Y1699C]LRRK2 Roc-COR mutants were purified from lysates of the infected *Sf*21 insect cells. Stoichiometries of Mg^{2+} co-purified with the LRRK2 Roc-COR (black bar) and [Y1699C]LRRK2 Roc-COR (grey bar) were determined by ICP-MS. The protein concentrations of the LRRK2 Roc-COR preparations were 12.3 – 12.5 µM and those of the [Y1699C]LRRK2 Roc-COR preparations ranged

from 6.6 – 8.1 μM. The concentrations of Mg^{2+} in the protein preparations were calculated from the raw ppb values as described in Supplemental Table S1. Stoichiometries (expressed as mol. Mg^{2+} per mol. of protein) of magnesium ion in the LRRK2 Roc-COR and [Y1699C]LRRK2 Roc-COR preparations are presented. Error bars indicate SEM of three replicate measurements.

B. Stoichiometry of Mg^{2+} co-purified with LRRK2 Roc-COR determined by ICP-AES. Recombinant LRRK2 Roc-COR in lysates of infected *Sf*9 cells was purified by Ni^{2+}-NTA agarose chromatography, dialyzed and subjected to ICP-AES, either alone or with addition of standards at 1, 0.1 and 0.01 mg/l. Measured intensity at the specified wavelength for magnesium ions were buffer-subtracted and converted to concentrations. The concentration of LRRK2 Roc-COR used was 1.93 ± 0.11μM. From the intensity of signal at the wavelength of 279.553 nm, the concentration of Mg^{2+} was calculated to be 2.05 ± 0.14 μM. Stoichiometry of Mg^{2+} bound to LRRK2 Roc-COR was determined from these concentrations. The error bar indicates SEM of three replicate measurements.

Figure 6 Effects of Y1699C mutation on the secondary structure contents, stability and GTPase activity of LRRK2 Roc-COR

A. The time course of release of ^{32}P inorganic phosphate generated by hydrolysis of [γ-^{32}P]GTP catalyzed by LRRK2 Roc-COR and [Y1699C]LRRK2 Roc-COR expressed in *Sf*21 cells. Data were calculated from at least three independent experiments (Error bars indicate ± SEM). B. The rates of GTP hydrolysis of LRRK2 Roc-COR and Rac1 determined by the GTPase activity assay (Error bars indicate ± SEM). C. Kinetic analysis of the GTPase activity of wild type LRRK2 Roc-COR. 12.3 pmol of purified recombinant LRRK2 Roc-COR protein expressed in *Sf*21 insect cells was used to perform the kinetic analysis (Error bars indicate ± SEM). **D.** Circular dichroism spectra of wild type LRRK2 Roc-COR and [Y1699C]LRRK2 Roc-COR expressed in *Sf21* insect cells. The table shows the secondary structure contents of LRRK2 Roc-COR and [Y1699C]LRRK2 Roc-COR estimated by the Bestsel prediction program. For the proportions of LRRK2 Roc-COR secondary structure contents, the α-helix is 13.7%, β-strand is 30.9% and others account for 55.4%. For the proportions of [Y1699C]LRRK2

Roc-COR secondary structure contents, the α-helix is 12.8%, β-strand is 33% and others account for 54.2%. **E.** Effects of the presence of different concentrations of guanidine hydrochloride on the secondary structure contents of LRRK2 Roc-COR and [Y1699C]LRRK2 Roc-COR determined by circular dichroism at wavelength of 222 nm. E. The denaturation profiles of two recombinant proteins.

References

Anand, V. S., Reichling, L. J., Lipinski, K. et al. (2009) Investigation of leucine-rich repeat kinase 2 : enzymological properties and novel assays. *Febs J.*, **276,** 466-478.

Biosa, A., Trancikova, A., Civiero, L., Glauser, L., Bubacco, L., Greggio, E. and Moore, D. J. (2013) GTPase activity regulates kinase activity and cellular phenotypes of Parkinson's disease-associated LRRK2. *Hum Mol Genet,* **22,** 1140-1156.

Bosgraaf, L. and Van Haastert, P. J. (2003) Roc, a Ras/GTPase domain in complex proteins. *Biochim Biophys Acta.,* **1643,** 5-10.

Chia, J. Y., Gajewski, J. E., Xiao, Y., Zhu, H. J. and Cheng, H. C. (2010) Unique biochemical properties of the protein tyrosine phosphatase activity of PTEN-demonstration of different active site structural requirements for phosphopeptide and phospholipid phosphatase activities of PTEN. *Biochim Biophys Acta,* **1804,** 1785-1795.

Civiero, L., Vancraenenbroeck, R., Belluzzi, E. et al. (2012) Biochemical characterization of highly purified leucine-rich repeat kinases 1 and 2 demonstrates formation of homodimers. *PLoS One,* **7,** e43472.

Dachsel, J. C., Nishioka, K., Vilarino-Guell, C. et al. (2010) Heterodimerization of Lrrk1-Lrrk2: Implications for LRRK2-associated Parkinson disease. *Mech Ageing Dev,* **131,** 210-214.

Daniels, V., Vancraenenbroeck, R., Law, B. M. et al. (2011) Insight into the mode of action of the LRRK2 Y1699C pathogenic mutant. *J Neurochem,* **116,** 304-315.

Deng, J., Lewis, P. A., Greggio, E., Sluch, E., Beilina, A. and Cookson, M. R. (2008) Structure of the ROC domain from the Parkinson's disease-associated leucine-rich

repeat kinase 2 reveals a dimeric GTPase. *Proc Natl Acad Sci U S A,* **105,** 1499-1504.

Deyaert, E., Wauters, L., Guaitoli, G. et al. (2017) A homologue of the Parkinson's disease-associated protein LRRK2 undergoes a monomer-dimer transition during GTP turnover. *Nat Commun,* **8,** 1008.

Doggett, E. A., Zhao, J., Mork, C. N., Hu, D. and Nichols, R. J. (2012) Phosphorylation of LRRK2 serines 955 and 973 is disrupted by Parkinson's disease mutations and LRRK2 pharmacological inhibition. *J Neurochem,* **120,** 37-45.

Floris, G., Cannas, A., Solla, P. et al. (2009) Genetic analysis for five LRRK2 mutations in a Sardinian parkinsonian population: importance of G2019S and R1441C mutations in sporadic Parkinson's disease patients. *Parkinsonism Relat Disord,* **15,** 277-280.

Foulkes, J. G., Howard, R. F. and Ziemiecki, A. (1981) Detection of a novel mammalian protein phosphatase with activity for phosphotyrosine. *FEBS Lett,* **130,** 197-200.

Gasper, R., Meyer, S., Gotthardt, K., Sirajuddin, M. and Wittinghofer, A. (2009) It takes two to tango: regulation of G proteins by dimerization. *Nat Rev Mol Cell Biol,* **10,** 423-429.

Gotthardt, K., Weyand, M., Kortholt, A., Van Haastert, P. J. and Wittinghofer, A. (2008) Structure of the Roc-COR domain tandem of C. tepidum, a prokaryotic homologue of the human LRRK2 Parkinson kinase. *EMBO J,* **27,** 2239-2249.

Guaitoli, G., Raimondi, F., Gilsbach, B. K. et al. (2016) Structural model of the dimeric Parkinson's protein LRRK2 reveals a compact architecture involving distant interdomain contacts. *Proc Natl Acad Sci U S A,* **113,** E4357-4366.

Guo, L., Gandhi, P. N., Wang, W., Petersen, R. B., Wilson-Delfosse, A. L. and Chen, S. G. (2007) The Parkinson's disease-associated protein, leucine-rich repeat kinase 2 (LRRK2), is an authentic GTPase that stimulates kinase activity. *Exp Cell Res.,* **313,** 3658-3670.

Hall, B. E., Bar-Sagi, D. and Nassar, N. (2002) The structural basis for the transition from Ras-GTP to Ras-GDP. *Proc Natl Acad Sci U S A,* **99,** 12138-12142.

Henry, A. G., Aghamohammadzadeh, S., Samaroo, H., Chen, Y., Mou, K., Needle, E. and Hirst, W. D. (2015) Pathogenic LRRK2 mutations, through increased kinase

activity, produce enlarged lysosomes with reduced degradative capacity and increase ATP13A2 expression. *Hum Mol Genet,* **24,** 6013-6028.

Ito, G. and Iwatsubo, T. (2012) Re-examination of the dimerization state of leucine-rich repeat kinase 2: predominance of the monomeric form. *Biochem J,* **441,** 987-994.

Ito, G., Okai, T., Fujino, G., Takeda, K., Ichijo, H., Katada, T. and Iwatsubo, T. (2007) GTP binding is essential to the protein kinase activity of LRRK2, a causative gene product for familial Parkinson's disease. *Biochemistry,* **46,** 1380-1388.

Kamikawaji, S., Ito, G., Sano, T. and Iwatsubo, T. (2013) Differential Effects of Familial Parkinson Mutations in LRRK2 Revealed by a Systematic Analysis of Autophosphorylation. *Biochemistry*.

Klein, C. L., Rovelli, G., Springer, W., Schall, C., Gasser, T. and Kahle, P. J. (2009) Homo- and heterodimerization of ROCO kinases: LRRK2 kinase inhibition by the LRRK2 ROCO fragment. *J Neurochem,* **111,** 703-715.

Lewis, P. A., Greggio, E., Beilina, A., Jain, S., Baker, A. and Cookson, M. R. (2007) The R1441C mutation of LRRK2 disrupts GTP hydrolysis. *Biochem Biophys Res Commun,* **357,** 668-671.

Li, X., Tan, Y. C., Poulose, S., Olanow, C. W., Huang, X. Y. and Yue, Z. (2007) Leucine-rich repeat kinase 2 (LRRK2)/PARK8 possesses GTPase activity that is altered in familial Parkinson's disease R1441C/G mutants. *J Neurochem,* **103,** 238-247.

Li, X., Wang, Q. J., Pan, N., Lee, S., Zhao, Y., Chait, B. T. and Yue, Z. (2011) Phosphorylation-dependent 14-3-3 binding to LRRK2 is impaired by common mutations of familial Parkinson's disease. *PLoS One,* **6,** e17153.

Li, Y., Dunn, L., Greggio, E., Krumm, B., Jackson, G. S., Cookson, M. R., Lewis, P. A. and Deng, J. (2009) The R1441C mutation alters the folding properties of the ROC domain of LRRK2. *Biochim Biophys Acta,* **1792,** 1194-1197.

Liao, J., Wu, C. X., Burlak, C. et al. (2014) Parkinson disease-associated mutation R1441H in LRRK2 prolongs the "active state" of its GTPase domain. *Proc Natl Acad Sci U S A,* **111,** 4055-4060.

Liu, M., Dobson, B., Glicksman, M. A., Yue, Z. and Stein, R. L. (2010) Kinetic mechanistic studies of wild-type leucine-rich repeat kinase 2: characterization of the kinase and GTPase activities. *Biochemistry,* **49,** 2008-2017.

Liu, M., Kang, S., Ray, S., Jackson, J., Zaitsev, A. D., Gerber, S. A., Cuny, G. D. and Glicksman, M. A. (2012) Kinetic, mechanistic, and structural modeling studies of truncated wild-type leucine-rich repeat kinase 2 and the G2019S mutant. *Biochemistry,* **50,** 9399-9408.

Liu, Z., Mobley, J. A., DeLucas, L. J., Kahn, R. A. and West, A. B. (2016) LRRK2 autophosphorylation enhances its GTPase activity. *FASEB J,* **30,** 336-347.

Marin, I., van Egmond, W. N. and van Haastert, P. J. (2008) The Roco protein family: a functional perspective. *FASEB J,* **22,** 3103-3110.

Mata, I. F., Wedemeyer, W. J., Farrer, M. J., Taylor, J. P. and Gallo, K. A. (2006) LRRK2 in Parkinson's disease: protein domains and functional insights. *Trends Neurosci,* **29,** 286-293.

Matta, S., Van Kolen, K., da Cunha, R. et al. (2012) LRRK2 controls an EndoA phosphorylation cycle in synaptic endocytosis. *Neuron,* **75,** 1008-1021.

Micsonai, A., Wien, F., Kernya, L., Lee, Y. H., Goto, Y., Refregiers, M. and Kardos, J. (2015) Accurate secondary structure prediction and fold recognition for circular dichroism spectroscopy. *Proc Natl Acad Sci U S A,* **112,** E3095-3103.

Mills, R. D., Mulhern, T. D., Cheng, H. C. and Culvenor, J. G. (2012) Analysis of LRRK2 accessory repeat domains: prediction of repeat length, number and sites of Parkinson's disease mutations. *Biochem Soc Trans,* **40,** 1086-1089.

Mills, R. D., Mulhern, T. D., Liu, F., Culvenor, J. G. and Cheng, H. C. (2014) Prediction of the repeat domain structures and impact of parkinsonism-associated variations on structure and function of all functional domains of leucine-rich repeat kinase 2 (LRRK2). *Hum Mutat,* **35,** 395-412.

Nichols, R. J., Dzamko, N., Morrice, N. A. et al. (2010) 14-3-3 binding to LRRK2 is disrupted by multiple Parkinson's disease-associated mutations and regulates cytoplasmic localization. *Biochem J,* **430,** 393-404.

Nixon-Abell, J., Berwick, D. C. and Harvey, K. (2016) L'RRK de Triomphe: a solution for LRRK2 GTPase activity? *Biochem Soc Trans,* **44,** 1625-1634.

Paisan-Ruiz, C., Jain, S., Evans, E. W. et al. (2004) Cloning of the gene containing mutations that cause PARK8-linked Parkinson's disease. *Neuron,* **44,** 595-600.

Poe, M., Scolnick, E. M. and Stein, R. B. (1985) Viral Harvey ras p21 expressed in Escherichia coli purifies as a binary one-to-one complex with GDP. *J Biol Chem,* **260,** 3906-3909.

Rudi, K., Ho, F. Y., Gilsbach, B. K., Pots, H., Wittinghofer, A., Kortholt, A. and Klare, J. P. (2015) Conformational heterogeneity of the Roc domains in C. tepidum Roc-COR and implications for human LRRK2 Parkinson mutations. *Biosci Rep,* **35**.

Sejwal, K., Chami, M., Remigy, H. et al. (2017) Cryo-EM analysis of homodimeric full-length LRRK2 and LRRK1 protein complexes. *Sci Rep,* **7,** 8667.

Sen, S., Webber, P. J. and West, A. B. (2009) Dependence of leucine-rich repeat kinase 2 (LRRK2) kinase activity on dimerization. *J Biol Chem,* **284,** 36346-36356.

Shutes, A. and Der, C. J. (2006) Real-time in vitro measurement of intrinsic and Ras GAP-mediated GTP hydrolysis. *Methods Enzymol,* **407,** 9-22.

Taymans, J. M., Vancraenenbroeck, R., Ollikainen, P., Beilina, A., Lobbestael, E., De Maeyer, M., Baekelandt, V. and Cookson, M. R. (2011) LRRK2 kinase activity is dependent on LRRK2 GTP binding capacity but independent of LRRK2 GTP binding. *PLoS One,* **6,** e23207.

Terheyden, S., Ho, F. Y., Gilsbach, B. K., Wittinghofer, A. and Kortholt, A. (2015) Revisiting the Roco G-protein cycle. *Biochem J,* **465,** 139-147.

Terheyden, S., Nederveen-Schippers, L. M. and Kortholt, A. (2016) The unconventional G-protein cycle of LRRK2 and Roco proteins. *Biochem Soc Trans,* **44,** 1611-1616.

Wittinghofer, A. and Vetter, I. R. (2011) Structure-function relationships of the G domain, a canonical switch motif. *Annu Rev Biochem,* **80,** 943-971.

Xiong, Y., Coombes, C. E., Kilaru, A., Li, X., Gitler, A. D., Bowers, W. J., Dawson, V. L., Dawson, T. M. and Moore, D. J. (2010) GTPase activity plays a key role in the pathobiology of LRRK2. *PLoS Genet.,* **6,** e1000902.

Xiong, Y., Yuan, C., Chen, R., Dawson, T. M. and Dawson, V. L. (2012) ArfGAP1 Is a GTPase Activating Protein for LRRK2: Reciprocal Regulation of ArfGAP1 by LRRK2. *J Neurosci,* **32,** 3877-3886.

Zhang, B., Zhang, Y., Wang, Z. and Zheng, Y. (2000) The role of Mg2+ cofactor in the guanine nucleotide exchange and GTP hydrolysis reactions of Rho family GTP-binding proteins. *J Biol Chem,* **275,** 25299-25307.

A.

B.

Names of constructs	Domains and affinity tags	Expression vectors & systems	Remarks on purity and expression level
GST- LRRK2 Roc-COR		pGEX6P3 *E. coli*	• Very low level of expression • HSP60 as major contaminant • data not shown
GST- LRRK2 Roc-COR		pFlacPAK9 *Sf*9 cells in complete Grace's medium	• Low level of expression • With a low molecular weight contaminant • data not shown
LRRK2 Roc-COR		pFlacPAK9 *Sf*9 in complete Grace's medium or *Sf*21 cells in serum-free medium	• Good level of expression • High purity after purification • Aggregate at high concentration • Figure 2
Short LRRK2 Roc-COR		pFlacPAK9 *Sf*9 in complete Grace's medium or *Sf*21 cells in serum-free medium	• Low level of expression • Low yield after Ni^{2+}-NTA agarose purification with many contaminants • Supplemental Figure S2
LRRK2 Roc-CORΔC		pFlacPAK9 *Sf*9 in complete Grace's medium or *Sf*21 cells in serum-free medium	• Good level of expression • Good yield after Ni^{2+}-NTA agarose purification but with many contaminants • Figure 3 and Supplemental Figure S5
[T1348N] LRRK2 Roc-COR		pFlacPAK9 *Sf*9 in complete Grace's medium or *Sf*21 cells in serum-free medium	• Low level of expression • Low yield after Ni^{2+}-NTA agarose purification with many contaminants • Data not shown
[Y1699C] LRRK2 Roc-COR		pFlacPAK9 *Sf*9 in complete Grace's medium or *Sf*21 cells in serum-free medium	• Good level of expression • High purity after purification • Aggregate at high concentration • Supplemental Figure S9

jnc_14566_f1.jpg

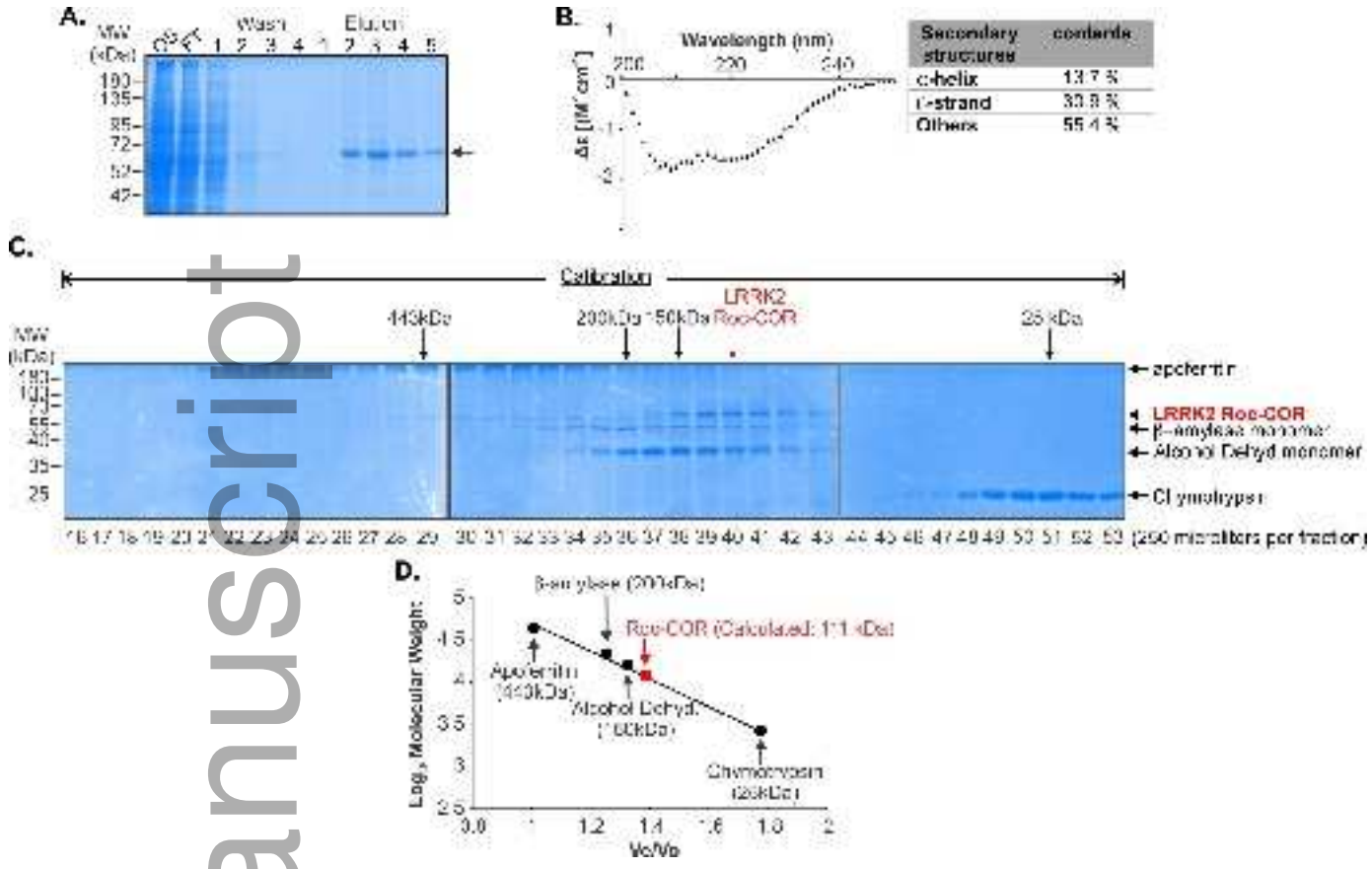

jnc_14566_f2.jpg

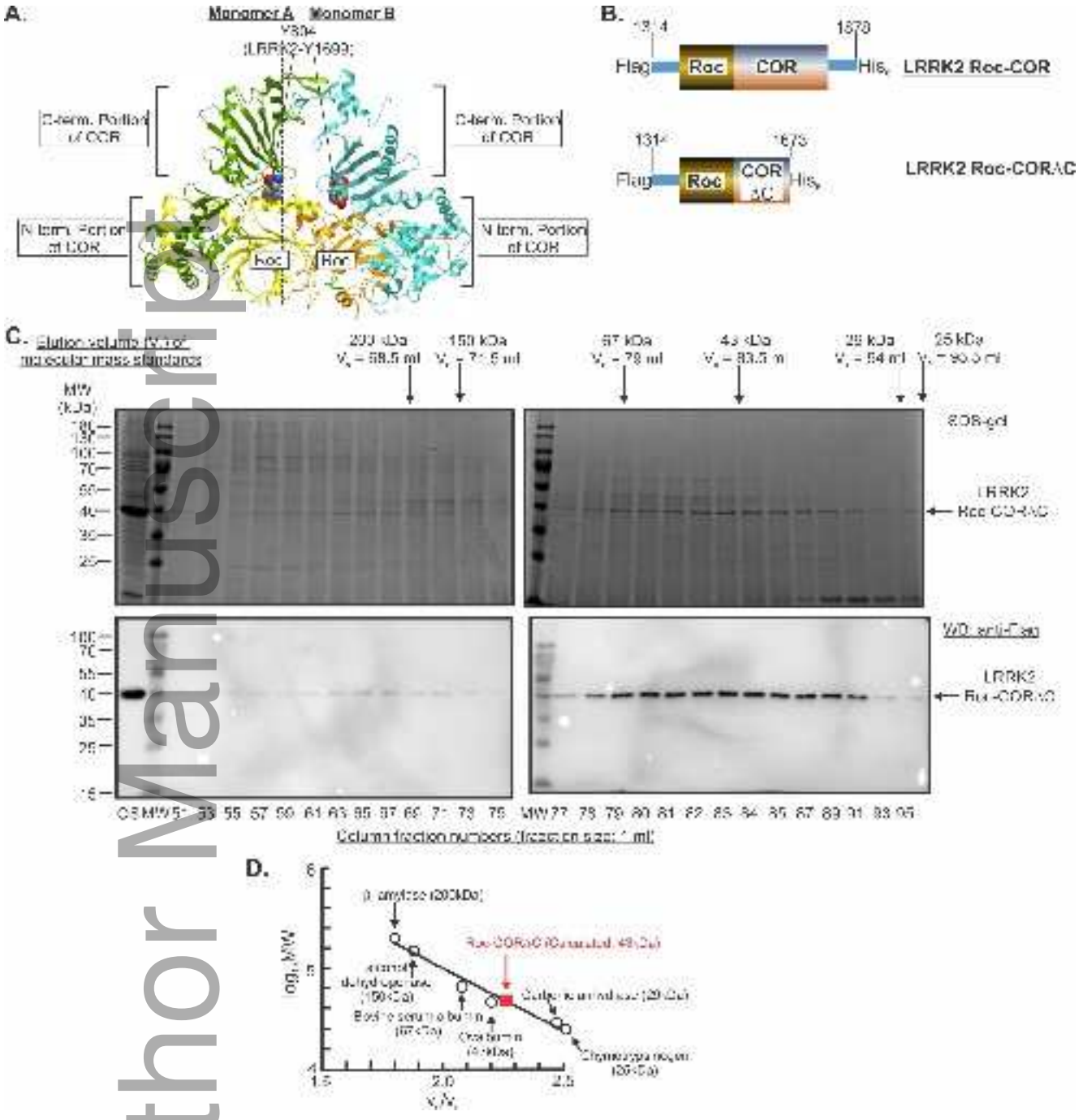

jnc_14566_f3.jpg

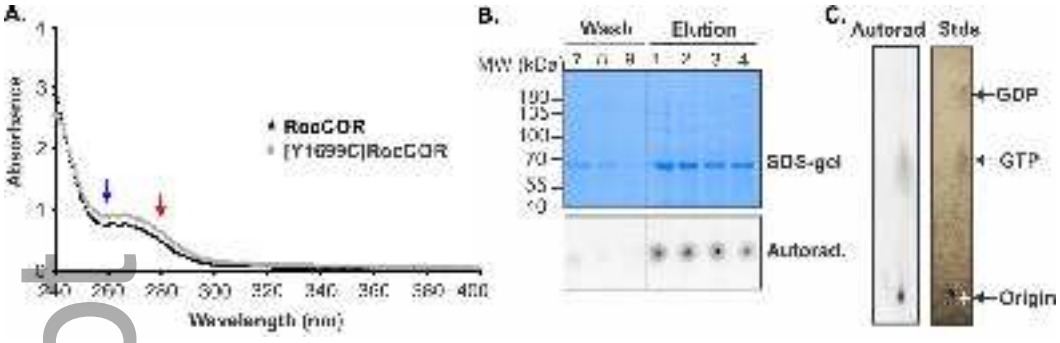

jnc_14566_f4.jpg

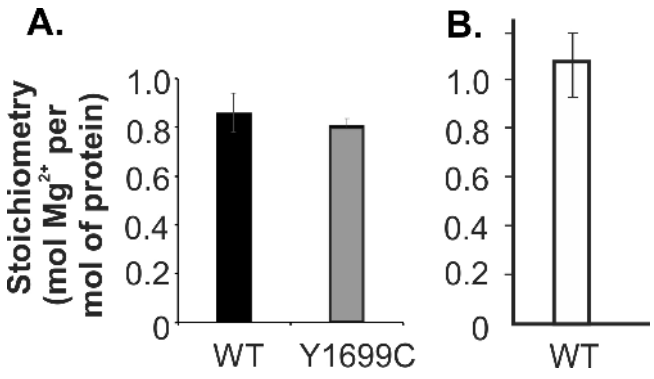

jnc_14566_f5.jpg

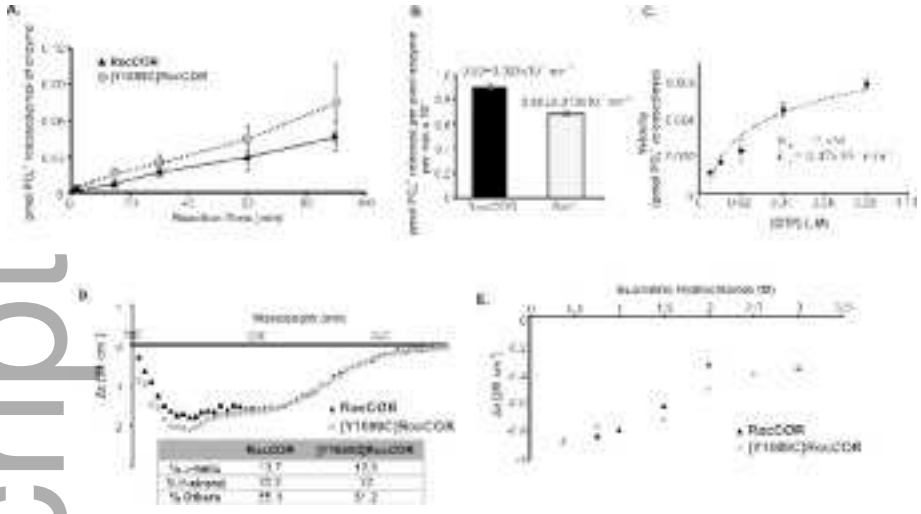

jnc_14566_f6.jpg